Integrating Spatial Pyramid Pooling for Multi-scale Brain Tumor Classification in Deep Learning

Karrar A. Kadhim[1], Ola N. Kadhim[2], and Fallah H. Najjar[3,4,*]

[1] Computer Techniques Engineering Department, Faculty of Information Technology, Imam Ja'afar Al-Sadiq University, Baghdad, Iraq
[2] Department of Medical Instruments Techniques, Technical Institute of Al-Mussaib, Al-Furat Al-Awsat Technical University, 51006 Babil, Iraq
[3] Department of Computer Networks and Software Techniques, Technical Institute of Najaf, Al-Furat Al-Awsat Technical University, 54001 Najaf, Iraq
[4] Faculty Department of Emergent Computing, Faculty of Computing, Universiti Teknologi Malaysia, 81310 UTM Johor Bahru, Johor, Malaysia
Email: karrar.abdulameer@ijsu.edu.iq (K.A.K.); ola.najah@atu.edu.iq (O.N.K.); fallahnajjar@atu.edu.iq (F.H.N.)
*Corresponding author

***Abstract*—Deep learning has transformed medical image analysis; in particular, many different brain tumors are being produced. Accurate detection is crucial for effective treatment and contributes to prolonging the life of patients. While MRI is a standard diagnostic tool, manual interpretation can be slow and sometimes error prone. As such, automatic classification systems based on Convolutional Neural Networks (CNNs) are gaining importance. However, standard CNNs are generally good for capturing only the continuous features within one region of the data, and that means they need huge amounts of training samples to work well in practice. We also struggle to capture diverse shapes, sizes and positions of brain tumors. To meet this challenge, our paper proposes the SPP-MobileNet model, which integrates a Spatial Pyramid Pooling (SPP) block into the MobileNet architecture. With the SPP layer for multi-scale feature extraction, our classifier is much better at spotting tumor appearance changes without resizing images. By building this into MobileNet, SPP-MobileNet maintains all that model's computational efficiency while boosting classification accuracy. On two Magnetic Resonance Imaging (MRI) datasets, the proposed model outperformed other state-of-the-art methods with an accuracy of 98.86% and perfect precision. Its recall rate was 97.68%, while the Matthews Correlation Coefficient value reached 97.75 %. These results suggest that SPP-MobileNet is a powerful tool for brain tumor classification, and it should go some way to improving diagnostic accuracy and speed. In the future, we will focus on tuning the model for more complex types of brain tumors and applying it across various other medical imaging tasks.**

***Keywords*— brain tumor classification, MRI image analysis, neuroimaging, SPP-MobileNet**

I. Introduction

Deep learning has revolutionized medical image analysis in recent years, particularly in classifying brain tumors [1, 2]. Brain tumors have a wide range of differences in size, shape and location [3]. They pose great challenges in diagnosis and treatment planning if not identified properly [4, 5]. Accurate detection and classification of these tumors are critical for effective treatment plans and for improving patient survival rates [6]. Traditionally, Magnetic Resonance Imaging (MRI) has been the standard for diagnosing brain tumors [7, 8].

Moreover, the risk of human error is always there. As a result, for several years, many people involved in scientific research have explored the possibility of developing systems to automatically classify these brain tumor data sets based on deep learning networks [5, 9, 10]. These systems have the potential to provide faster, more accurate diagnoses, thus aiding clinicians when they make clinical decisions [11, 12]. Convolutional Neural Networks (CNNs), deep-learning models, have performed remarkably in various image classification tasks [13, 14]. They learn hierarchical features from raw images and are very suitable for medical applications in image processing [15]. CNNs can be successfully used for multiple functions, such as detecting diabetic retinopathy, classifying skin lesions and identifying lung cancers from CT scans [16]. For example, within brain tumor classification, CNNs can be used to distinguish between different tumor types like gliomas, meningiomas and pituitary tumors. However, CNN-based models are still faced with many difficulties in this field. Because every patient and MRI modality has inherent variables, getting

Manuscript received November 27, 2024; revised January 21, 2025; accepted March 6, 2025; Published July 17, 2025.

equally successful results across all situations and data types is hard [17, 18].

Our main contributions are as follows: (i) Integrating the Spatial Pyramid Pooling (SPP) block into the MobileNet architecture (SPP-MobileNet) enables the model to capture multi-scale features effectively from MRI images, managing such issues as size, shape, and location differences among tumors. Combining SPP with MobileNet further enhances the generalization characteristics of the model. It can now seafood features at several different scales and positions simultaneously, increasing its accuracy rating in classification without needing an image to be rescaled or cropped. (ii) In addition to a more complicated SPP layer, the addition of SPP still allows the model to keep MobileNet's computational efficiency: It contains a Depthwise Separable Convolutional architecture.

II. Literature Review

Brain tumor localization is essential to medical diagnosis, which plays a role in accurate diagnosis and effective treatment planning [2, 6]. Radiological imaging techniques do not earn responsibility for this. Great improvements have been made [19]. Brain tumor diagnosis is one of the most challenging problems of its kind. It is difficult because tumors can take on many shapes and appearances in an MRI scan [20, 21]. It is essentially slow-growing and well-defined, whereas high-grade tumors are diffuse, large and invasive [22]. Because of this variation in size, shape intensity and location within the brain, standard CNN designs with fixed-size receptive fields have difficulty capturing all relevant features for accurate classification [12, 22].

Furthermore, MRI signal intensities differ according to the specific sequence (e.g., T1-weighted or FLAIR image) [23]. The appearance and anatomic structure variations of MR images affect the interpretation model [24]. Therefore, they must be able to cope with these differences often among patients and even at different hospitals. Thirdly, a problem arises from the scarcity of annotated medical data [25]. Thus, deep learning models need large amounts of labeled data for good performance in a medical setting. However, collecting large, well-annotated datasets in the medical field is often difficult due to the need for expert annotations [26]. This process is both time-intensive and costly.

Furthermore, in volume, the incidence of brain tumors is relatively low compared with other cancers, and distribution among different tumor types is nonuniform [27]. Consequently, some tumor types are considerably more common than others; it is not balanced data [28, 29]. This lack of balance can cause models that are strong on common tumor types but weak at the classification of rare ones [29]. Consequently, we need various ways to solve these problems to improve the brain tumor classification model's generalization ability [30]. However, in brain tumor classification, the paramount obstacle is to build a model that can handle the variation in tumor appearance across different patients and MRI modalities effectively while at the same time maintaining high accuracy [31, 32]. These traditional CNN models have fixed receptive fields, which are insufficient to capture the all-scale nature of brain tumors and thus deliver suboptimal performance [33]. In addition, the scarcity of annotated medical data and the imbalance in types of tumors exacerbate the difficulty in constructing a robust, generalized model [34]. Thus, a better approach is needed to capture multi-scale features from MRI images while circumventing the data constraints routinely encountered in medical image classification tasks [35, 36].

However, this statement is challenged by manual analysis. As large volumes of data and complex visual details are involved in MRI scans, it takes great skill to perform this task, which can take hours or even days. Therefore, automatic MRI must be taken up as it will greatly enhance efficiency and accuracy [24]. Although much previous research has been devoted to developing machine learning models for brain tumor detection, these models are often trained on relatively small datasets [37]. Unable to handle the transfer learning task, such models cannot achieve high accuracy and reliability in some cases. This issue underscores the need to develop more robust techniques to cope with larger and more complex datasets for better model results. Several approaches have been proposed that combine preprocessing, extracting features and classification [38].

For example, Woodbright *et al.* [39] address the critical issue of interpretability in deep learning models, specifically in the context of medical applications. In these cases, knowing what decisions are made transparently is essential. Their work introduces the Autonomous Relevance Technique for Explainable Neurological Disease Prediction (ART-Explain). Their system automatically extracts features of deep learning architectures to offer entirely new visual explanations for predictions. In the high stakes of incorrect diagnoses with neurological conditions, where errors significantly affect morbidity and mortality, the need for such transparent models is the greatest. ART-Explain is an attempt to provide an end-to-end solution that gives intuitive human-oriented overviews of predictions, enhancing trust and understanding for its users. They report the method's performance on three data sets for neurological disorders, concluding with 98.32% accuracy, 98.34% recall and 98.27% specificity. Najeih *et al.* [40] have contributed significantly to the field of brain tumor classification using deep learning models, specifically focusing on improving the accuracy of automatic detection and diagnosis in medical imaging. Their research emphasizes using CNNs and other deep learning architectures to enhance the precision of tumor classification based on MRI images. Like other contemporary studies, Najeih *et al.* [40] leveraged pre-trained models such as VGG16, ResNet, and DenseNet, building on their ability to automatically extract relevant features from complex medical images. In a key study, Najeih *et al.* [40] incorporated a variety of image preprocessing techniques, including filtering and contrast enhancement, to improve image quality before feeding the data into deep learning models. This approach aligns with

the methods used in other studies, such as the current research, which also integrates preprocessing techniques like Kuwahara filtering and homomorphic sharpening to boost the visibility of key structures within MRI images. By enhancing the clarity of tumor regions, Najeih *et al.*'s methodology [40] increases the accuracy of classification, particularly when distinguishing between tumor types like glioma, meningioma, and pituitary tumors.

Zhang *et al.* [41] have taken up the challenge of grading meningiomas, which will be measured according to peritumoral edema regions. In their approach, they integrate radiomic and deep learning techniques. Their work embodies a transfer learning-based engineering of the Meningioma Feature Extraction Model (MFEM), which combines the virtues of both Vision Transformer (ViT) and CNN architectures for better feature extraction. It is worth noting that they draw later attention to an often-neglected area: the PTE region, Nonsense behind which can be higher-grade tumors. The method performed well, achieving a grading accuracy rate of 92.86%, and precision, sensitivity and specificity were 93.44%, 95% and 89.47%, respectively, for a data set with 98 patients. Their findings suggest that incorporating radionics and deep learning into preoperative meningioma grading to combat inter-aural variability effectively improves the accuracy of preoperative diagnosis and minimizes observer errors, which will offer direct help for clinical decision-making.

Ibrahim *et al.* [42] explore the potential of CNNs in classifying MRI images, particularly for Alzheimer's disease detection and brain tumor identification. While CNNs have demonstrated significant potential, optimizing their parameters remains a challenge due to the complexity of the search space, often leading to suboptimal results. This limitation necessitates trial-and-error methods and expert judgment in parameter tuning, which can hinder the development of real-world applications. To address this issue, the authors proposed a hybrid model that combines Particle Swarm Optimization (PSO) with CNNs to optimize hyper-parameters more effectively. The PSO algorithm was employed to determine the optimal configuration of CNN parameters, which are then applied to the CNN architecture for improved classification accuracy. The hybrid model was evaluated using three benchmark datasets. The results demonstrate the model's superiority, achieving accuracy, precision, and recall rates of 97.12, 92.66, and 99.02, respectively, thereby highlighting the effectiveness of PSO in enhancing CNN performance for MRI image classification. To improve the performance of machine learning models used for tumor diagnosis, Shilaskar *et al.* [43] looked into various preprocessing techniques designed to eliminate noise from MRI images, ensuring that doctors have accurate information to work on.

Further input to the strength of model feature extraction techniques they developed is always based on textures, gradient-based descriptor types, and even the tiny overall shakes and jiggles of their systems, such as histograms of movement directions. An effective feature extraction process was seminal in successfully classifying machine learning models. Perhaps XGBoost consistently performs better than other algorithms because it engages in ensemble learning techniques. This result suggests that ensemble learning techniques, such as XGBoost, offer a promising path forward in automating brain tumor detection, providing doctors with an ever more reliable and efficient diagnosis tool.

III. Materials and Methods

MobileNet architecture is the foundation of the proposed model, structured as a series of Depthwise separable convolutions. This architecture efficiently reduces computational complexity while maintaining performance. The input to the model is an MRI image I of size H×W×3, where H and W represent the height and width of the image, and 3 refers to the RGB color channels.

This study introduces the SPP-MobileNet model for brain tumor classification by integrating the SPP layer into the MobileNet architecture. The model is designed to extract multi-scale features effectively from MRI images of brain tumors, enhancing classification accuracy across diverse tumor types. However, we extend the MobileNet architecture, displayed in Fig. 1, with the SPP-MobileNet model shown in Fig. 2.

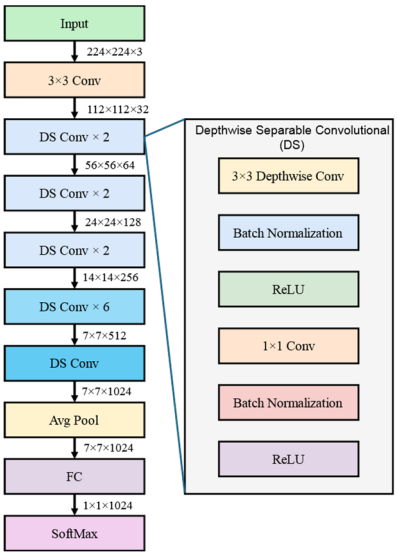

Fig. 1. Backbone MobileNet architecture.

The initial convolutional layers of MobileNet apply a series of filters to the input image, extracting features as:

$$X = f(W ** I) \tag{1}$$

where X is the feature map, W represents filter weights, $**$ denotes convolution, and f is a non-linear activation function such as ReLU (Rectified Linear Unit). These layers output feature maps with reduced spatial dimensions and increased depth, capturing high-level features from the input image.

The core enhancement of the proposed model is the inclusion of the SPP layer, which allows for multi-scale feature extraction. The SPP layer performs spatial pyramid pooling at multiple levels, allowing the model to generate fixed-length feature vectors from input images of variable

sizes. The SPP layer applies pooling operations at different scales, with pooling sizes defined as $P_1, P_2, \ldots, P_n$.

For each pooling scale P_i, the input feature map X is partitioned into non-overlapping blocks, each of size $\frac{H}{P_i} \times \frac{W}{P_i}$. The pooling operation within each block can be represented as:

$$X_{P_i} = MaxPool(X, P_i) \tag{2}$$

where X_{P_i} is the output of the pooling operation for scale P_i, and $MaxPool$ is the MaxPooling function. The result is a downsampled representation of the feature map at each scale.

Each pooled feature map X_{P_i} is then flattened into a vector and concatenated with the other pooled feature vectors across the scales:

$$SPP(X) = Flatten(X_{P_i}) \oplus \ldots \oplus Flatten(X_{P_n}) \tag{3}$$

where $\oplus$ represents vector concatenation. The output of the SPP layer is a fixed-length vector regardless of the input size, which contains multi-scale information crucial for capturing diverse tumor sizes and shapes.

The concatenated feature vector from the SPP layer is passed through a series of fully connected layers for classification. Let the output of the SPP layer be denoted as Z_{SPP}. The first fully connected layer applies a linear transformation followed by a non-linear activation function.

$$Z_1 = f(W_1 Z_{SPP} + b_1) \tag{4}$$

where Z_1 is the output of the fully connected layer, W_1 and b_1 are the weights and biases of the layer, and f is the ReLU activation function:

$$f(x) = \max(0, x) \tag{5}$$

Next, a dropout layer is applied to reduce overfitting during training. The output from the first fully connected layer is transformed into:

$$Z_1^{'} = \text{Dropout}(Z_1, p) \tag{6}$$

where p is the dropout probability, this prevents the model from overly relying on any subset of neurons during training.

Finally, the output is passed through another fully connected layer with a SoftMax activation function to generate the final classification scores for the C classes:

$$\hat{y} = \text{SoftMax}(W_2 Z_1^{'}, b_2) \tag{7}$$

The SoftMax function converts the raw logits into probabilities for each class:

$$\text{SoftMax}(z_i) = \frac{\exp(z_i)}{\sum_{j=1}^{C} \exp(z_i)} \tag{8}$$

The utilization of Depthwise separable convolutions distinguishes the latter. These convolution layers are intended to reduce the computational complexity of the model while maintaining a high level of accuracy. MobileNet takes the input MRI images through a series of lightweight convolution operations, drawing out spatial features and reducing the spatial dimensions of the image while increasing data depth for that image.

This enhancement will set the scene for feature extraction of the classification problem and allow the model to efficiently handle the rich and complex information present in human brain tumor MRI images in a very robust manner. The core innovation of the proposed model lies in integrating the SPP block into MobileNet, as shown in Fig. 2.

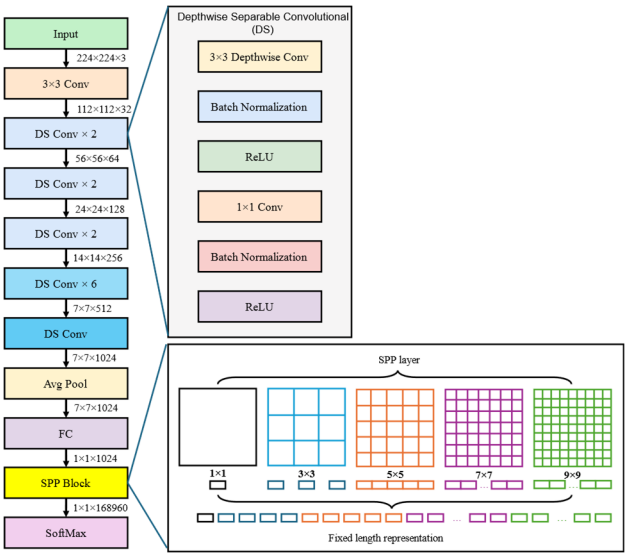

Fig. 2. The proposed SPP-MobileNet architecture.

The SPP Layer allows the model to capture multi-scale features by performing max-pooling on the feature maps at different levels spatially. A different scale of pooling divides the feature map into non-overlapping blocks, taking the maximum value in each block.

This method makes the model capable of producing fixed-size feature vectors, no matter how big the input image is. MRI is a very important property because it may have pictures that vary in resolution from poor to sufficient. That feature vector helps the train camper the model to classify different tumor types and sizes effectively. In Figs. 3 and 4, we highlight the structure of our customized SPP block, which enhances the original SPP, Fig. 3, by adding more refined pooling operations and concatenation strategies.

This block produces multi-scale features, $(1 \times 1), (3 \times 3), (5 \times 5), (7 \times 7)$, and (9×9) vectors fed into fully connected layers for classification. The SPP block contributes to the model's robustness by key spatial information at different resolutions, thus boosting classification accuracy. Introducing this SPP block preserving allows the SPP-MobileNet model to generalize better across various types of brain tumors, applying more

powerful tools in medical image analysis by using these golden features that span multiple scales.

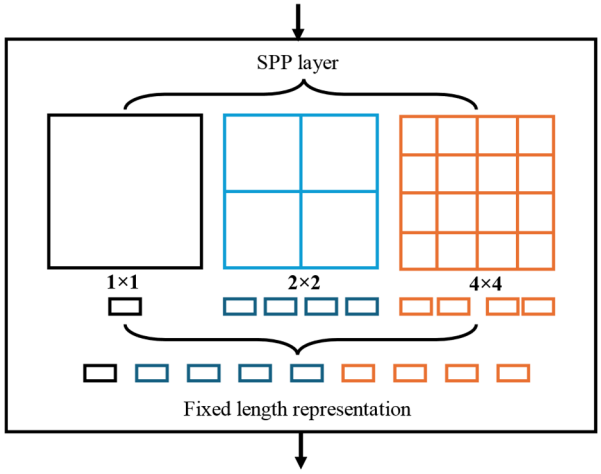

Fig. 3. Original SSP block.

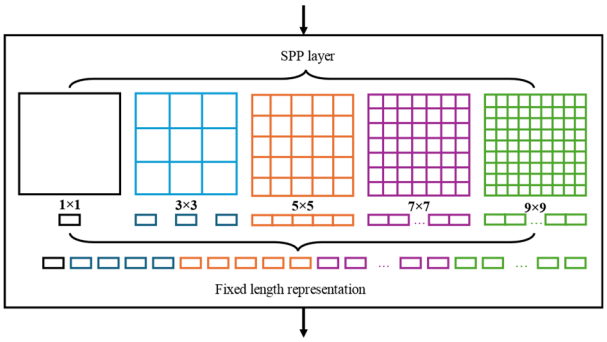

Fig. 4. Our proposed SSP block.

Furthermore, the model is designed to handle input images resized to 224×224 pixels and can handle multi-class and binary classification problems. It is trained for 20 epochs with a batch size of 32. the learning rate was tuned to 0.0001. The optimizer used for optimization is Adam, and cross-entropy is the loss function. The model uses accuracy as the primary metric when evaluating performance. These hyper-parameters define the training process and allow for a comprehensive assessment of model performance.

However, the performance of the proposed model is evaluated using standard classification metrics, including accuracy, precision, recall, F1-score, and the Matthews Correlation Coefficient (MCC). These metrics are computed as follows [18, 44, 45]:

$$Accuracy = \frac{\text{TP+TN}}{TP+TN+FP+FN} \tag{9}$$

$$Precision = \frac{\text{TP}}{TP+FP} \tag{10}$$

$$Recall = \frac{\text{TP}}{TP+FN} \tag{11}$$

$$F1 = \frac{2 \times Precision \times Recall}{Precision+Recall} \tag{12}$$

$$Specificity = \frac{TN}{TN+FP} \tag{13}$$

$$MCC = \frac{(TP \times TN)-(FP \times FN)}{\sqrt{(TP+FP)(TP+FN)(TN+FP)(TN+FN)}} \tag{14}$$

where TP and FP represent the true and false positives, respectively, TN and FN represent the true and false negatives.

IV. Result and Discussion

In this section, we present the performance of our proposed model, which integrates the SPP layer into the MobileNet architecture for brain tumor classification. The model was evaluated on two MRI datasets: Brain Tumor MRI Datasets [46], displayed in Fig. 5, and Brain Tumor Dataset [47], presented in Fig. 6. The Brain Tumor MRI Dataset consists of 7023 MRI images of human brains and can be divided into four types: glioma, meningioma, no tumor, and pituitary tumors. This dataset was gathered from a variety of sources. Among them are the figshare, the SARTAJ, and the Br35H datasets. One interesting fact about it is that all the pictures in the tumor class were drawn from Br35H, which means there is an equal chance of having no brain tumors. Images in this dataset vary in scale, complexity and type of Tumor, giving us a rich source for multi-class tumor classification. Brain Tumor Dataset: This binary class dataset of 5264 MRI images. NoTumor contains 2500 images, while Tumor comprises 2764. It focuses on solving the binary classification problem and distinguishing between Tumor and NoTumor conditions.

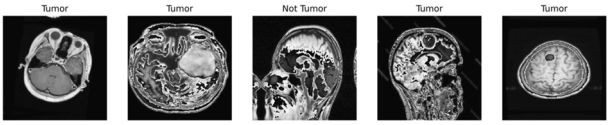

Fig. 5. Brain tumor dataset samples [46].

Fig. 6. Brain tumor MRI dataset samples [47].

Further, the binary dataset was divided into three subgroups: 80% training, 10% validation, and 10% testing. The Brain Tumor MRI Dataset has already been split into training and testing sets. The training set contains 5702 images across four classes: glioma (1321), meningioma (1339), no tumor (1595), and pituitary tumors (1457). The testing set includes a total of 1311 images distributed across the four classes as follows: glioma (300), meningioma (306), no tumor (405), and pituitary tumors (300). The authors split the training set into training 90% and validation 10%.

To make the model more robust and avoid overfitting, we employed various data enhancement techniques on training data via a semi-automatic pipeline. We used a flow of data augmentation techniques based on the training phase. These techniques included normalization, resizing images to match the input size of models, random flip (horizontal), random rotation at a 0.02 factor and random scaling with a magnitude up to 20%. These transformed photographs increase model accuracy and generalization capabilities by adding statistical artificial noise into the training set. A simpler data augmentation pipeline was used for the validation and test data. It involves only normalizing and resizing, leaving all random transformations aside. This way, the validation and testing frameworks can accurately evaluate models on real-world data scales. To ensure that the normalization layers were adjusted based on the training data for universal uniform scaling across all datasets.

We will now present the outcome of training and validation of four deep learning models, our proposed SPP-MobileNet, the backbone MobileNet, ResNet, and AlexNet—using the Brain Tumor dataset, a collection of MRI images labeled under two classes of normal (i.e., no tumor) and abnormal (i.e., having a brain tumor).

As for AlexNet, Fig. 7, with results contributing to a reasonable level of performance, has lagged while maintaining this simpler type of architecture that is easier to build and comprehend. By this measure, it reaches its maximum accuracy at 98%.

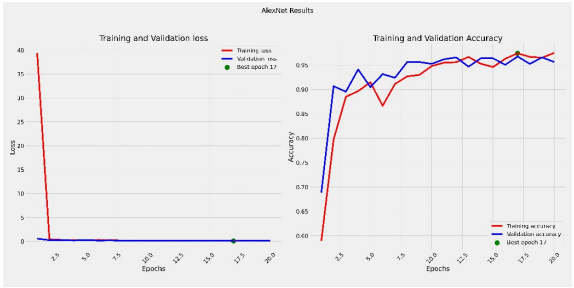

Fig. 7. AlexNet training and validation loss and accuracy regarding the brain tumor dataset.

ResNet, Fig. 8, achieves good results with this dataset at some times but has unstable performance, with wildly swinging validation loss, which is also attributed to fluctuations in accuracy.

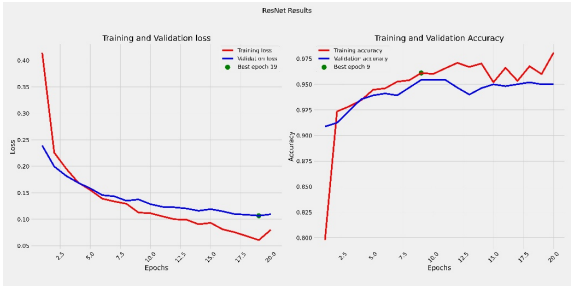

Fig. 8. ResNet training and validation loss and accuracy regarding the brain tumor dataset.

As shown in Figs. 9 and 10, the best performance score is the SPP-MobileNet model, in which both the training and validation accuracy reached 99 percent and very low final loss values prevailed, see Fig. 10. This is due to SPP Blocking enabling the capture of multi-scale spatial features, which are critical for identifying tumors of varying sizes in the brain. MobileNet, on the other hand, Fig. 9, still displays good abilities in this context, is slightly less accurate in its validation and achieves 96% recognition rates. Its efficient construction provides opportunities for improvement here and simultaneously eliminates the SPP block that previously played such a crucial role in extracting features on different scales.

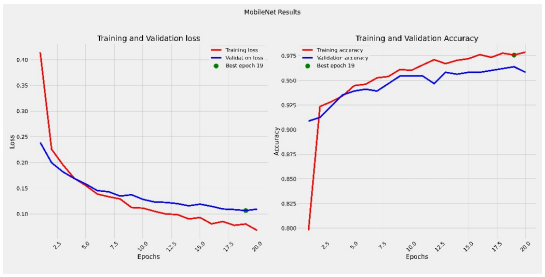

Fig. 9. Backbone MobileNet training and validation loss and accuracy regarding the brain tumor dataset.

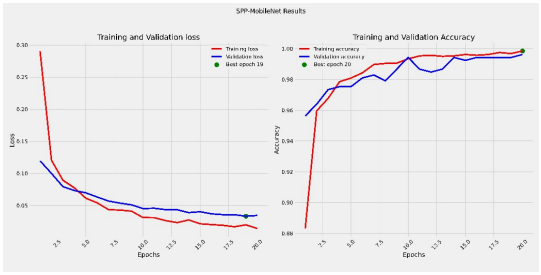

Fig. 10. Our proposed SSP-MobileNet training and validation loss and accuracy regarding the brain tumor dataset.

This implies that the intricate dynamics of this dataset may call for further adjustment or an alternative approach on ResNet.

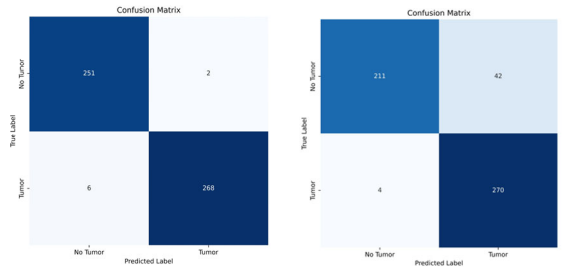

Fig. 11. Confusion Matrix: (left) AlexNet and (right) ResNet.

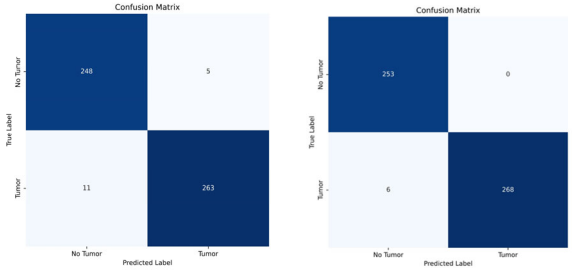

Fig. 12. Confusion Matrix: (left) MobileNet and (right) SSP-MobileNet.

From Figs. 11 and 12, SPP-MobileNet gives the best results in brain tumor detection in the confusion matrix. When it comes to brain tumor identification, even a few mistakes in judging whether a test sample contains tissue from any source other than a tumor or nontumor test. The benefits of using SPP block for multi-scaling feature extraction in medical images. AlexNet and MobileNet also achieve high performance. The gap between their results and those of SPP-MobileNet suggests that state-of-the-art features, such as the SPP block, should be built into model architectures. ResNet, however, exhibits great limitations in that it overfits the model. The result is an unacceptably high rate of false positives. Thus, SPP-MobileNet is the most powerful and best model for this dataset. This makes it a promising tool in brain tumor detection and diagnosis. Furthermore, the performance metrics of our proposed SPP-MobileNet, the backbone MobileNet, ResNet, and AlexNet are shown in Table I.

TABLE I. COMPARATIVE ANALYSIS OF PROPOSED SPP-MOBILENET WITH STATE-OF-THE-ART TECHNIQUES REGARDING THE BRAIN TUMOR DATASET

Metrics	AlexNet [48]	ResNet [49, 50]	MobileNet [51]	SPP-MobileNet
Accuracy	98.48%	91.27%	96.96%	**98.86%**
Precision	99.21%	83.40%	98.02%	**100%**
Recall	97.67%	**98.14%**	95.75%	97.68%
F1	98.43%	90.17%	96.88%	**98.83%**
Specificity	99.26%	86.54%	98.13%	**100%**
MCC	96.97%	83.30%	93.95%	**97.75%**

According to performance metrics in Table I, SPP-MobileNet, other models on brain tumor classification were tested by comparison for outperforming all of them. It has high accuracy and a low false positive rate. It possesses strong generalization abilities as well. However, all these suggest that it promises good medical applications particularly where brain tumors must be diagnosed with an MRI image. Its feature extraction capabilities of lessening the feature volume enable the model to employ complex and multi-scale characteristics in medical imaging data easily. This ability is rather significant since such characteristics complicate more than anything else as a medical technology manufacturer not in any sense least because MRI images are a case in point.

Furthermore, the performance of the proposed SPP-MobileNet model was evaluated using another dataset, the Brain Tumor MRI Dataset, which includes four classes: glioma, meningioma, no tumor, and pituitary Tumor. The results are presented using a confusion matrix and training and validation loss and accuracy curves, demonstrating the model's effectiveness in classifying brain tumors. Fig. 13. Displays the and training and validation loss and accuracy curves, while Fig. 14. shows the confusion matrix of the proposed SPP-MobileNet.

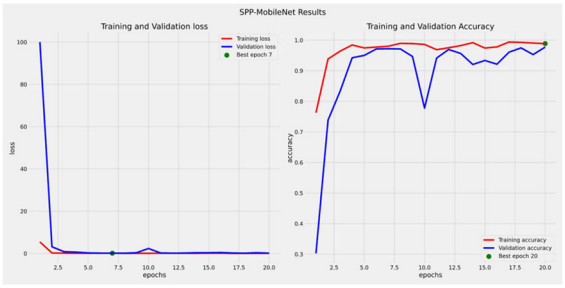

Fig. 13. Our proposed SSP-MobileNet training and validation loss and accuracy regarding the brain tumor MRI dataset.

The training and validation loss curves in Fig. 8 show that both losses decreased rapidly during the first few epochs and stabilized near-zero values after the seventh epoch. By the 20th epoch, both losses were consistently low, with little difference between them. This trend suggests that the model learns quickly and efficiently without overfitting. The close training and validation loss indicate generalization to validation sets: SPP-MobileNet is robust enough on unobserved data retention and has powerful predictivity capabilities.

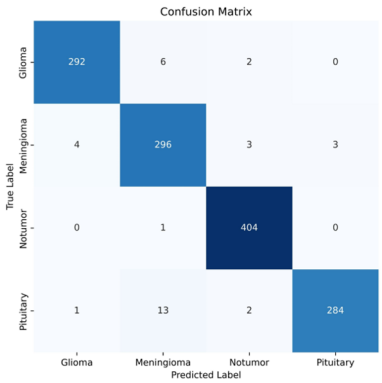

Fig. 14. Our proposed SSP-MobileNet confusion matrix regarding the brain tumor MRI dataset.

From the results, we can conclude that SPP-MobileNet performs exceptionally well on the Brain Tumor MRI Dataset. It has high accuracy and achieves class-leading performance for all these tumors. From the confusion matrix, the model distinguishes between no-tumor and tumor cases. High cumulative classification precision suggests that the SPP block's fast convergence makes multi-scale feature extraction by the model itself work very well. These results show that SPP-MobileNet, though it may suffer a slight misclassification between meningioma and pituitary tumors, is a very good model for brain tumor classification and performs excellently on this dataset. Moreover, Table II provides the results of the SPP-MobileNet model of the Brain Tumor MRI Dataset from Table I, including key performance metrics such as accuracy, precision, recall, specificity, and F1-score for each brain tumor type: meningioma, pituitary tumors, non-tumor, part of the brain or glial cell cancer on any depth level; and, finally, pituitary tumors. In short, this gives us an average value across all aspects rather than just by category.

TABLE II. SPP-MOBILENET RESULTS REGARDING THE BRAIN TUMOR MRI DATASET

Classes	Accuracy	Precision	Recall	F1	Specificity
Glioma	99.01	97.33	98.32	97.82	99.51
Meningioma	97.71	96.73	93.67	95.18	98.01
No Tumor	99.39	99.75	98.30	99.02	99.23
Pituitary	98.55	94.67	98.95	96.76	99.70
Average	98.67	97.12	97.31	97.20	99.11

We can see from Table II that SPP-MobileNet has achieved high accuracy for all four classes. The model does well even in a challenging environment, with very high accuracy on MRI images. The score for meningioma and pituitary tumors is less than no tumor and glioma, a sign that more work remains to raise these values; nonetheless, overall, the model shows its exceptional reliability and accuracy. It is a highly recommended alternative for the medical image classification task based on deep learning CNN, not just because of its smooth and powerful performance. SPP-MobileNet boasts overwhelming accuracy rates and an x-hard-like condition with no tumor.

Nevertheless, both meningioma and pituitary tumors collect very low scores, hinting that we could adjust the model's error rates by fine-tuning there; this method has very good reliability and achieves a considerable success rate. These figures express what was already found through the confusion matrix and training/validation accuracy. I have further confirmed that the methodology is robust. Finally, we compare our proposed SPP-MobileNet with state-of-the-art methods.

Table III comprehensively compares different models for MRI image classification. These efforts especially concentrated on recognized benchmarks in brain tumor identification. From the models above, concerning most of the indexes mentioned, our SPP-MobileNet achieves the highest of any other model. Its accuracy is up to 98.67%, precision attains 97.12%, recall rates 97.31%, and the F1-Score 97.20%. Further, with a remarkable specificity level of 99.11%, it is obvious that this model is not only skillful at accurately telling true negatives from false ones but also possesses high-tech abilities for preventing many types of misidentifications.

TABLE III. COMPARATIVE ANALYSIS OF THE SPP-MOBILENET WITH STATE-OF-THE-ART TECHNIQUES REGARDING THE BRIAN TUMOR MRI DATASET

Author, Ref	Accuracy	Precision	Recall	F1	Specificity
Nigjeh *et al.* (VGG19) [40]	93.00	92.75	92.50	92.50	-
Nigjeh *et al.* (DenseNet) [40]	93.00	93.25	93.00	93.25	-
Nigjeh *et al.* (ResNet) [40]	91.00	91.00	90.75	87.50	-
Ibrahim *et al.* [42]	97.12	92.66	**99.02**	-	-
Woodbright *et al.* [39]	98.32	-	98.34	-	98.27
Shilaskar *et al.* [43]	92.02	92.07	91.82	91.85	-
Our SPP-MobileNet	**98.67**	**97.12**	97.31	**97.20**	**99.11**

Nigjeh *et al.* [40] compare three data pictures (VGG19-DenseNet-ResNet) architectures under wide-ranging data conditions. Results of their model: success was invariable over VGG19 and Dense net, 93% either way. The ResNet model, however, performed worse with an accuracy of 91% and an F1-Score that showed a dramatic dip to 87.50%. This indicates that ResNet has difficulty achieving a good balance between both sides, leading it into valleys where everything fluctuates up and down perforce. Ibrahim *et al.* introduced a combined model of CNN and PSO.

That model achieved an accuracy of 97.12% and a recall of 99.02. However, the precision rate is so low-just 92.66%; it seems to show that there may be some tradeoffs between identifying truly infected cases when false alarms also rank higher. Woodbright *et al.* achieved high recall (98.34%) and specificity (98.27%), relative to an overall accuracy of 98.32%, as it can catch most true positives and negatives.

However, only the latter was characterized in the manuscript; no other metrics like precision or F1-Score are reported for this system, which restricts our ability to estimate its performance more fully compared with the above steps. Shilaskar *et al.* [43] have more decent scores of 92.02% accuracy, 92.07% precision and 91.82 % recall, respectively. The F1-Score of 91.85% indicates that the tradeoff between precision and recall is quite stable, though not on par with most other models.

Furthermore, the performance of SPP-MobileNet is superior in the following discussion section. Its speed drops slowly as it enters bigger and bigger scales of tumors, but clarity is high apart from that. However, some limitations also need to be considered. One of these is the misclassification between meningiomas and pituitary tumors, even though future developments include improving the model specifically for these tough cases and enlarging its applicability to all kinds of medical imaging tasks.

V. CONCLUSION

This study introduced the integration of the SPP block into the MobileNet for brain tumor classification. This integration allows the MobileNet model to capture multi-stage appearances over a single patient in terms of different sizes, shapes and locations of brain tumors, which is very challenging and has never been achieved by traditional attention mechanisms. By adding the SPP layer, the model excels in accuracy and generalization between various tumor types and, therefore, is strongly fitting for medical image classification tasks. Indeed, results reveal that SPP-MobileNet significantly outperforms other state-of-the-art deep learning models and the baseline MobileNets. The model also keeps MobileNet's low computational overhead, allowing for an efficient algorithm in a clinical setting. Although it appeared that the study does have merits, some limitations surrounding this study were noted. The model did not achieve the same high level of accuracy in differentiating between meningiomas and pituitary tumors, so further optimization is needed for some tumor types. Moreover, like many deep learning models, SPP-MobileNet needs far more annotated medical data to

perform at these levels. The lack of such data and potential bias in the available datasets could affect the generalization of this model to larger patient populations and clinical settings.

In future work, more optimizations can concentrate on increasing model performance on distinct, challenging-to-classify tumor types like meningiomas and pituitary tumors. Researchers may also investigate methods to alleviate the potential for input sparsity, such as utilizing transfer learning or synthetic data augmentation to improve training. Generalizing the model to other medical imaging tasks, like detecting various neurological conditions, would extend its clinical relevance and importance.

CONFLICT OF INTEREST

The author declares that there are no conflicts of interest to report regarding the present study.

AUTHOR CONTRIBUTIONS

K.A.K conceptualization, methodology, investigation, visualization, writing—original draft, data curation. O.N.K. supervision, formal analysis, validation, and resources, Writing—review and editing, writing the final draft. F.H.N. writing, reviewing, editing, methodology, project administration, validation, resources, writing reviews, supervision, data curation, formal analysis, validation, and resources. All authors had approved the final version.

REFERENCES

[1] M. W. Nadeem *et al.*, "Brain tumor analysis empowered with deep learning: A review, taxonomy, and future challenges," *Brain Sciences*, vol. 10, no. 2, p. 118, 2020. https://doi.org/10.3390/brainsci10020118

[2] R. Ranjbarzadeh, A. Caputo, E. B. Tirkolaee, S. J. Ghoushchi, and M. Bendechache, "Brain tumor segmentation of MRI images: A comprehensive review on the application of artificial intelligence tools," *Computers in Biology and Medicine*, vol. 152, 106405, 2023. https://doi.org/10.1016/j.compbiomed.2022.106405

[3] K. Sailunaz, S. Alhajj, T. Özyer, J. Rokne, and R. Alhajj, "A survey on brain tumor image analysis," *Medical & Biological Engineering & Computing*, vol. 62, no. 1, pp. 1–45, 2024. https://doi.org/10.1007/s11517-023-02873-4

[4] N. Kazimierczak, W. Kazimierczak, Z. Serafin, P. Nowicki, J. Nożewski, and J. Janiszewska-Olszowska, "AI in orthodontics: Revolutionizing diagnostics and treatment planning—A comprehensive review," *Journal of Clinical Medicine*, vol. 13, no. 2, p. 344, 2024. https://doi.org/10.3390/jcm13020344

[5] Z. Amiri, A. Heidari, N. J. Navimipour, M. Esmaeilpour, and Y. Yazdani, "The deep learning applications in IoT-based bio-and medical informatics: A systematic literature review," *Neural Computing and Applications*, vol. 36, no. 11, pp. 5757–5797, 2024. https://doi.org/10.1007/s00521-023-09366-3

[6] S. Khalighi, K. Reddy, A. Midya, K. B. Pandav, A. Madabhushi, and M. Abedalthagafi, "Artificial intelligence in neuro-oncology: Advances and challenges in brain tumor diagnosis, prognosis, and precision treatment," *NPJ Precision Oncology*, vol. 8, no. 1, p. 80, 2024. https://doi.org/10.1038/s41698-024-00575-0

[7] A. Batool and Y.-C. Byun, "Brain tumor detection with integrating traditional and computational intelligence approaches across diverse imaging modalities-Challenges and future directions," *Computers in Biology and Medicine*, 108412, 2024. https://doi.org/10.1016/j.compbiomed.2024.108412

[8] R. Ranjbarzadeh, A. B. Kasgari, S. J. Ghoushchi, S. Anari, M. Naseri, and M. Bendechache, "Brain tumor segmentation based on deep learning and an attention mechanism using MRI multi-modalities brain images," *Scientific Reports*, vol. 11, no. 1, pp. 1–17, 2021. https://doi.org/10.1038/s41598-021-90428-8

[9] M. Güler and E. Namlı, "Brain tumor detection with deep learning methods' classifier optimization using medical images," *Applied Sciences*, vol. 14, no. 2, p. 642, 2024. https://doi.org/10.3390/app14020642

[10] M. Aljohani *et al.*, "An automated metaheuristic-optimized approach for diagnosing and classifying brain tumors based on a convolutional neural network," *Results in Engineering*, vol. 23, 102459, 2024. https://doi.org/10.1016/j.rineng.2024.102459

[11] K. Neamah *et al.*, "Brain tumor classification and detection based DL models: A systematic review," *IEEE Access*, 2023. https://doi.org/10.1109/ACCESS.2023.3347545

[12] M. A. Rahman *et al.*, "GliomaCNN: An effective lightweight CNN Model in assessment of classifying brain tumor from magnetic resonance images using explainable AI," *CMES-Computer Modeling in Engineering & Sciences*, vol. 140, no. 3, 2024. https://doi.org/10.32604/cmes.2024.050760

[13] K. Neamah, F. Mohamed, S. R. Waheed, W. H. M. Kurdi, A. Yaseen, and K. A. Kadhim, "Utilizing deep improved ResNet50 for brain tumor classification based MRI," *IEEE Open Journal of the Computer Society*, 2024. https://doi.org/10.1109/OJCS.2024.3453924

[14] I. M. Madhat, K. N. Kadhim, F. Mohamed, M. S. M. Rahim, F. H. Najjar, and A. J. Ramadhan, "Diagnosing Alzheimer's disease severity: A comparative study of deep learning algorithms," in *Proc. BIO Web of Conferences*, vol. 97: EDP Sciences, 2024, p. 00102. https://doi.org/10.1051/bioconf/20249700102

[15] J. Ker, L. Wang, J. Rao, and T. Lim, "Deep learning applications in medical image analysis," *IEEE Access*, vol. 6, pp. 9375–9389, 2017. https://doi.org/10.1109/ACCESS.2017.2788044

[16] H. Jiang *et al.*, "A review of deep learning-based multiple-lesion recognition from medical images: classification, detection and segmentation," *Computers in Biology and Medicine*, vol. 157, 106726, 2023. https://doi.org/10.1016/j.compbiomed.2023.106726

[17] F. Altaf, S. M. Islam, N. Akhtar, and N. K. Janjua, "Going deep in medical image analysis: Concepts, methods, challenges, and future directions," *IEEE Access*, vol. 7, pp. 99540–99572, 2019. https://doi.org/10.1109/ACCESS.2019.2929365

[18] F. H. Najjar, A. A. AbdulAmeer, and S. Kadum, "Hybrid SVD and SURF-based framework for robust image forgery detection and object localization," *Journal of Robotics and Control (JRC)*, vol. 6, no. 2, pp. 535–542, 2025. https://doi.org/10.18196/jrc.v6i2.25567

[19] R. Najjar, "Redefining radiology: A review of artificial intelligence integration in medical imaging," *Diagnostics*, vol. 13, no. 17, p. 2760, 2023. https://doi.org/10.3390/diagnostics13172760

[20] S. Y. Kandimalla, D. M. Vamsi, S. Bhavani, and M. VM, "Recent methods and challenges in brain tumor detection using medical image processing," *Recent Patents on Engineering*, vol. 17, no. 5, pp. 8–23, 2023. https://doi.org/10.2174/1872212117666220823100209

[21] S. Solanki, U. P. Singh, S. S. Chouhan, and S. Jain, "Brain tumor detection and classification using intelligence techniques: An overview," *IEEE Access*, vol. 11, pp. 12870–12886, 2023. https://doi.org/10.1109/ACCESS.2023.3242666

[22] L. Ugga *et al.*, "Neoplasms and tumor-like lesions of the sellar region: Imaging findings with correlation to pathology and 2021 WHO classification," *Neuroradiology*, vol. 65, no. 4, pp. 675–699, 2023. https://doi.org/10.1007/s00234-023-03120-1

[23] V. Velej, K. Cankar, and J. Vidmar, "The effects of normobaric and hyperbaric oxygenation on MRI signal intensities T_1-weighted, T_2-weighted and FLAIR images in human brain," *Radiology and Oncology*, vol. 57, no. 3, pp. 317–324, 2023. https://doi.org/10.2478/raon-2023-0043

[24] Z. Chen, K. Pawar, M. Ekanayake, C. Pain, S. Zhong, and G. F. Egan, "Deep learning for image enhancement and correction in magnetic resonance imaging—State-of-the-art and challenges," *Journal of Digital Imaging*, vol. 36, no. 1, pp. 204–230, 2023. https://doi.org/10.1007/s10278-022-00721-9

[25] M. Mirmozaffari and N. Kamal, "The application of data envelopment analysis to emergency departments and management of emergency conditions: A narrative review," in *Healthcare*, vol. 11, no. 18, 2023, p. 2541. https://doi.org/10.3390/healthcare11182541

[26] R. Jiao *et al.*, "Learning with limited annotations: A survey on deep semi-supervised learning for medical image segmentation," *Computers in Biology and Medicine*, 107840, 2023. doi: https://doi.org/10.1016/j.compbiomed.2023.107840
[27] F. Girardi *et al.*, "Global survival trends for brain tumors, by histology: Analysis of individual records for 556,237 adults diagnosed in 59 countries during 2000–2014 (CONCORD-3)," *Neuro-oncology*, vol. 25, no. 3, pp. 580–592, 2023. https://doi.org/10.1093/neuonc/noac217
[28] M. T. Ramakrishna, V. K. Venkatesan, I. Izonin, M. Havryliuk, and C. R. Bhat, "Homogeneous adaboost ensemble machine learning algorithms with reduced entropy on balanced data," *Entropy*, vol. 25, no. 2, p. 245, 2023. https://doi.org/10.3390/e25020245
[29] E. Vorontsov *et al.*, "A foundation model for clinical-grade computational pathology and rare cancers detection," *Nature Medicine*, pp. 1–12, 2024. https://doi.org/10.1038/s41591-024-03141-0
[30] Z. Liu *et al.*, "Deep learning based brain tumor segmentation: A survey," *Complex & Intelligent Systems*, vol. 9, no. 1, pp. 1001–1026, 2023.
[31] J. Alyami *et al.*, "Tumor localization and classification from MRI of brain using deep convolution neural network and Salp swarm algorithm," *Cognitive Computation*, vol. 16, no. 4, pp. 2036–2046, 2024. https://doi.org/10.1007/s12559-022-10096-2
[32] K. K. Kumar *et al.*, "Brain tumor identification using data augmentation and transfer learning approach," *Computer Systems Science & Engineering*, vol. 46, no. 2, 2023. https://doi.org/10.32604/csse.2023.033927
[33] Q. Li, B. Sun, and B. Bhanu, "Lite-FENet: Lightweight multi-scale feature enrichment network for few-shot segmentation," *Knowledge-Based Systems*, vol. 278, 110887, 2023. https://doi.org/10.1016/j.knosys.2023.110887
[34] Y. Yang, H. Zhang, J. W. Gichoya, D. Katabi, and M. Ghassemi, "The limits of fair medical imaging AI in real-world generalization," *Nature Medicine*, pp. 1–11, 2024. https://doi.org/10.1038/s41591-024-03113-4
[35] C. Lin, Y. Chen, S. Feng, and M. Huang, "A multibranch and multiscale neural network based on semantic perception for multimodal medical image fusion," *Scientific Reports*, vol. 14, no. 1, p. 17609, 2024. https://doi.org/10.1038/s41598-024-68183-3
[36] T. Mahmood, A. Rehman, T. Saba, L. Nadeem, and S. A. O. Bahaj, "Recent advancements and future prospects in active deep learning for medical image segmentation and classification," *IEEE Access*, 2023. https://doi.org/10.1109/ACCESS.2023.3313977
[37] S. Saeedi, S. Rezayi, H. Keshavarz, and S. R. N. Kalhori, "MRI-based brain tumor detection using convolutional deep learning methods and chosen machine learning techniques," *BMC Medical Informatics and Decision Making*, vol. 23, no. 1, p. 16, 2023. https://doi.org/10.1186/s12911-023-02114-6
[38] F. H. Najjar, N. B. Hassan, and S. Abd Kadum, "Hybrid deep learning model for hippocampal localization in Alzheimer's diagnosis using U-Net and VGG16," *International Journal of Robotics and Control Systems*, vol. 5, no. 2, pp. 730–747, 2025. https://doi.org/10.31763/ijrcs.v5i2.1739
[39] M. D. Woodbright, A. Morshed, M. Browne, B. Ray, and S. Moore, "Towards transparent AI for neurological disorders: A feature extraction and relevance analysis framework," *IEEE Access*, 2024. https://doi.org/10.1109/ACCESS.2024.3375877
[40] M. K. Nigjeh, H. Ajami, A. Mahmud, M. S. U. Hoque, and S. E. Umbaugh, "Comparative analysis of deep learning models for brain tumor classification in MRI images using enhanced preprocessing techniques," in *Applications of Digital Image Processing XLVII*, vol. 13137, SPIE, 2024, pp. 48–52. https://doi.org/10.1117/12.3028318
[41] H. Zhang *et al.*, "Deep learning model for the automated detection and histopathological prediction of meningioma," *Neuroinformatics*, vol. 19, pp. 393–402, 2021. https://doi.org/10.1007/s12021-020-09492-6
[42] R. Ibrahim, R. Ghnemat, and Q. A. Al-Haija, "Improving Alzheimer's disease and brain tumor detection using deep learning with particle swarm optimization," *AI*, vol. 4, no. 3, pp. 551–573, 2023. https://doi.org/10.3390/ai4030030
[43] S. Shilaskar, T. Mahajan, S. Bhatlawande, S. Chaudhari, R. Mahajan, and K. Junnare, "Machine learning based brain tumor detection and classification using HOG feature descriptor," in *Proc. 2023 International Conference on Sustainable Computing and Smart Systems (ICSCSS)*, 2023, pp. 67–75. https://doi.org/10.1109/ICSCSS57650.2023.10169700
[44] K. A. Kadhim, F. Mohamed, F. H. Najjar, G. A. Salman, and A. J. Ramadhan, "Localizing the thickness of cortical regions to descriptor the vital factors for Alzheimer's disease using UNET deep learning," in *Proc. BIO Web of Conferences*, vol. 97: EDP Sciences, 2024, p. 00054. https://doi.org/10.1051/bioconf/20249700054
[45] F. H. Najjar, S. A. Kadum, and N. B. Hassan, "Integrating multi-scale feature extraction into EfficientNet for acute lymphoblastic leukemia classification," *Journal of Image and Graphics*, vol. 13, no. 1, pp. 83–89, 2025. https://doi.org/10.18178/joig.13.1.83-89
[46] M. Nickparvar. Brain tumor MRI dataset. [Online]. Available: https://www.kaggle.com/datasets/masoudnickparvar/brain-tumor-mri-dataset
[47] V. Patel. Brain tumor dataset. [Online]. Available: https://www.kaggle.com/datasets/vishwapatel10/brain-tumor-dataset
[48] A. Krizhevsky, I. Sutskever, and G. E. Hinton, "Imagenet classification with deep convolutional neural networks," *Advances in Neural Information Processing Systems*, vol. 25, 2012. https://doi.org/10.1145/3065386
[49] S. Targ, D. Almeida, and K. Lyman, "Resnet in resnet: Generalizing residual architectures," arXiv preprint arXiv:1603.08029, 2016. https://doi.org/10.48550/arXiv.1603.08029
[50] B. Koonce and B. Koonce, "ResNet 50," *Convolutional Neural Networks with Swift for Tensorflow: Image Recognition and Dataset Categorization*, pp. 63–72, 2021. https://doi.org/10.1007/978-1-4842-6168-2
[51] A. G. Howard, "Mobilenets: Efficient convolutional neural networks for mobile vision applications," arXiv preprint arXiv:1704.04861, 2017.